CODEN:LUTEDX/(TEIE-7289)/1-18/(2021)

Industrial Electrical Engineering and Automation

Soft sensors for the return sludge flow rate in the Henriksdal MBR process

Hanna Molin

Division of Industrial Electrical Engineering and Automation
Faculty of Engineering, Lund University

Soft sensors for the return sludge flow rate in the Henriksdal MBR process

October 15, 2021

Contents

Abbreviations and variables

Abbreviation	Explanation
MBR	Membrane bioreactor
HRT	Hydraulic retention time
RAS	Return activated sludge
SRT	Sludge retention time
WAS	Waste activated sludge
WWTP	Wastewater treatment plant

Variable	Explanation	Unit
A_{bio}	Bioreactor surface area	m^2
H	Pressure head	m
h_{bio}	Water level in the bioreactor	m
h_{RAS}	Water level in the RAS pump tank	m
h_{ref}	Reference height, height of crest of the weir	m
L	Length of the weir	m
$MLSS$	Mixed liquor suspended solids	g/m^3
μ	Coefficient, accounts for friction loss	-
n	Number of revolutions	-
P	Power	W
Q	Flow rate	m^3 /s
Q_{bio}	Incoming flow rate	m^3 /s
Q_{DMB}	RAS flow rate calculated from dynamic mass balance	m^3 /s
Q_{mean}	Mean of the four RAS flow rate estimates	m^3 /s
Q_{median}	Median of the four RAS flow rate estimates	m^3 /s
Q_{pump}	RAS flow rate calculated from pump model	m^3 /s
Q^*_{pump}	RAS flow rate from the control system	m^3 /s
Q_{RAS}	RAS flow rate	m^3 /s
Q_{SMB}	RAS flow rate calculated from static mass balance	m^3 /s
Q_{tot}	Total outgoing flow rate from bioreactor	m^3 /s
Q_{WAS}	WAS flow rate	m^3 /s
Q_{weir}	RAS flow rate calculated over weir	m^3 /s
SS_{RAS}	Suspended solids in the RAS flow	g/m^3
V_{bio}	Bioreactor volume	m^3

1 Introduction

The Henriksdal wastewater treatment plant (WWTP) in Stockholm, Sweden, has undergone a massive rebuild in recent years. Facing both an increasing population and stricter effluent requirements, the owner Stockholm Vatten och Avfall (SVOA) needed to increase the capacity and the effectiveness of the treatment plant. In addition, one of SVOA's other WWTPs, Bromma, is to be terminated and the wastewater will instead be treated at Henriksdal WWTP. The WWTP is situated underground, which makes it difficult to extend the area of the treatment plant. SVOA therefore decided to implement a relatively new and compact treatment process - Membrane Bioreactor (MBR). Henriksdal WWTP will be one of the world's largest wastewater treatment facility using MBR once it is finalized. By 2040, the treatment plant will treat wastewater from 1 621 000 people, with an average daily influent flow rate of 530 000 $m^3/d = 6.13\ m^3/s$ (Stockholm Vatten och Avfall, 2017).

1.1 The treatment process

The total incoming flow is split in seven separate lines. The primary treatment consists of screens, sandtraps, and a primary settler. The biological treatment process at Henriksdal WWTP consists of a MBR process with pre and post denitrification (Figure 1). Before the wastewater enters the biological treatment, it is filtered in a fine screen to reduce solids. This is needed to avoid build up of coarse material and debris in the MBR. The wastewater then enters the anoxic zone where pre denitrification occurs. Each treatment line has two flexible zones that can be aerated or not. After the flex zones, there is an aerated zone followed by a deoxidation zone where external carbon is added to stimulate denitrification.

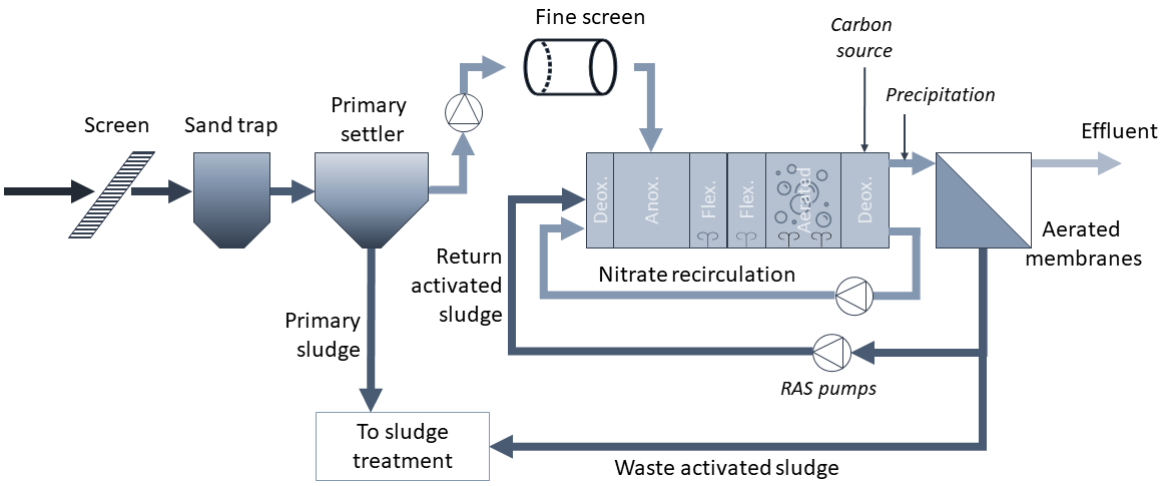

Figure 1. Simple overview of the treatment process.

In a traditional activated sludge plant, the sludge is separated in secondary settlers whereas at Henriksdal WWTP, these are replaced with aerated membranes. The membranes consist of hollow fibres that efficiently remove suspended solids from the effluent by filtration, and can achieve very low suspended solids concentrations in the effluent (Hammer and

Hammer, 2014; Stockholm Vatten och Avfall, 2017). The membranes are aerated to prevent clogging and fouling. The sludge is withdrawn from the bottom of the membrane tank. Part of the settled sludge is recirculated as return activated sludge (RAS). The excess sludge, or waste activated sludge (WAS) is thickened and digested to produce biogas. The RAS flow is pumped, with a lift height of approximately 1 m, back to the deoxidation zone.

The MBR process has, just like an activated sludge process, the benefit that the hydraulic retention time (HRT) and the sludge retention time (SRT) are separated and the goal should be to have a longer SRT than the HRT. The conditions in such a process allows for both rapid and slow growing microorganisms to thrive, which in turn affect the BOD removal, nitrogen removal, and the sludge characteristics. It also makes it possible to control the sludge age, which is important for nitrogen removal (la Cour Jansen et al., 2019).

The sludge concentration in the aerated zone should be kept stable and constant as an average over time, which is controlled by the excess sludge rate (Q_{WAS}). Q_{RAS} controls the partitioning between the membrane tank and the bioreactor. It is undesirable to have a large build up of sludge in the MBR tank. Furthermore, Q_{RAS} has a major impact on the treatment performance so Q_{RAS} must be estimated as good as possible to be able to analyze the overall performance. The energy consumption of the RAS pumps is a major part of the total energy consumption. For advanced control of the RAS pumps, it is beneficial to have a robust measurement or estimate of the flow rate. The MBR process is the most energy consuming part of the treatment plant, where the aeration of the membranes has the highest energy demand followed by the 56 RAS pumps (8 RAS pumps for each of the 7 lines).

1.2 Objective

The RAS flow rate is difficult to measure in the real plant due to physical constraints. It is instead estimated based on the pumps' characteristics and the frequency they are currently operated at. The objective of this study is to evaluate other methods to estimate Q_{RAS} to create a soft sensor that can be used to analyze performance and for advanced control of the RAS pumps. Several estimates of Q_{RAS} will be evaluated and compared. A possible benefit with this is redundancy in the soft sensor. In the future it may also be possible to use the different calculations for fault detection and/or predictive maintenance. This is, however, not included in this study.

This study will focus on line 1 of the WWTP as it is currently being deployed but can easily be extended to include several lines.

2 Estimating the return activated sludge flow rate

Monitoring and control of wastewater treatment processes are essential for well functioning treatment plants that are resource efficient and comply with effluent requirements. On-line and off-line analysis of a number of process variables; flow rates, concentrations of nitrogen (ammonia, nitrates, and total nitrogen), phosphorous (phosphates and total phosphorous), suspended solids, biochemical and chemical oxygen demand amongst others, is the core of monitoring. However, some process variables may be hard or impossible to monitor in a reliable way, either due to lack of equipment or physical constraints at the treatment plant. Thus arises a need for other ways of monitoring. Known relations and well-monitored variables can be used to estimate other process variables - i.e. soft-sensors.

Soft-sensors have been vastly used in wastewater treatment and process control (see e.g. Haimi et al. (2013) and the references therein). The soft sensor model can either be a mechanistic model that makes use of known relations between monitored variables to estimate non-monitored variables, or models developed using multivariate methods (Mali and Laskar, 2020), or neural networks (Pisa et al., 2019) and other machine learning techniques such as decision trees or k-Nearest neighbor (del Olmo et al., 2019).

This study relies on known relations between the variables in use, further described in the following sections. All simulations were done using an MBR model of Henriksdal WWTP based on the Benchmark Simulation Model no. 2 (BSM2) and its underlying models with minor modifications.

2.1 Dynamic mass balance

Two of the fundamental laws of physics are that mass and energy can not be destroyed, they can only transfer into different forms. The mass that is accumulated in a system must therefore equal the sum of mass entering the system and the mass that is produced within the system, minus the mass that leaves the system and that is consumed within the system:

$$\text{Accumulation} = \text{Inflow} + \text{Production} - \text{Consumption} - \text{Outflow}$$

In terms of the bioreactor, the mass balance is simplified by assuming that the outgoing mass is zero (no suspended solids in the effluent, $SS_{eff} = 0$), and that the waste sludge flow rate is much smaller than the return sludge flow rate ($Q_{WAS} << Q_{RAS}$) and therefore negligible. The growth and decay are assumed to compensate for each other and can thereby be neglected. The mass balance can then be simplified to only cover the bioreactor (dashed line in Figure 2).

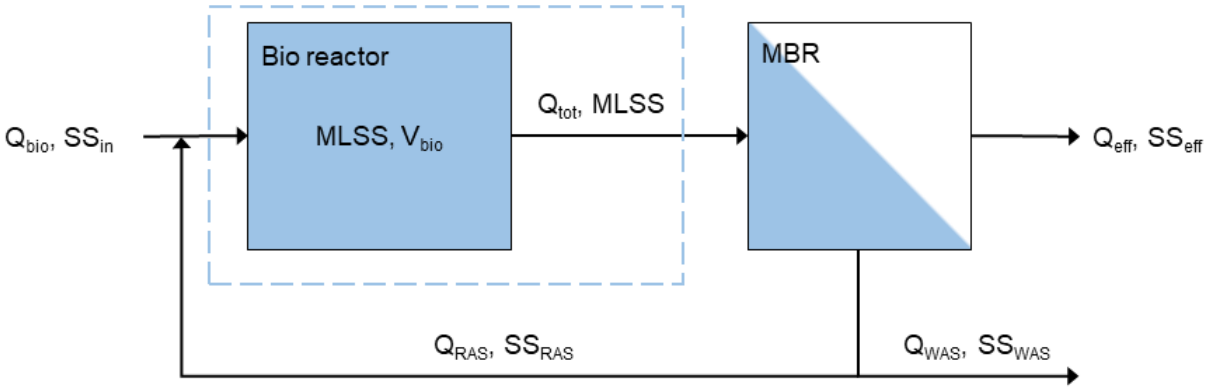

Figure 2. Illustration of the system over which the mass balance was defined.

The change in mass in the bioreactor, $d(SS_{bio} * V_{bio})/dt$, is given by (1)

$$\frac{d(SS_{bio} * V_{bio})}{dt} = Q_{bio}SS_{in} + Q_{RAS}SS_{RAS} - Q_{tot}SS_{bio} \tag{1}$$

where SS_{in} is assumed to be zero. Applying the product rule for derivatives on (1) yields

$$\frac{d(SS_{bio} * V_{bio})}{dt} = V_{bio}\frac{dSS_{bio}}{dt} + SS_{bio}\frac{dV_{bio}}{dt} \tag{2}$$

Equations (1) and (2) give (with the assumption that $SS_{in} = 0$)

$$Q_{RAS}SS_{RAS} - Q_{tot}SS_{bio} = V_{bio}\frac{dSS_{bio}}{dt} + SS_{bio}\frac{dV_{bio}}{dt} \tag{3}$$

where the suspended solids concentration in the bioreactor is the mixed liqour suspended solids concentration $MLSS$ ($SS_{RAS} = MLSS$).

Furthermore, the change in volume is defined by the differences in incoming and outgoing flow rates,

$$\frac{dV_{bio}}{dt} = Q_{bio} + Q_{RAS} - Q_{tot} \tag{4}$$

Using (4) in (2) and solving for $dMLSS/dt$ results in

$$\frac{dMLSS}{dt} = \frac{1}{V_{bio}}\left(Q_{RAS}SS_{RAS} - (Q_{bio} + Q_{RAS})\,MLSS\right) \tag{5}$$

where Q_{bio}, $MLSS$ and SS_{RAS} are observations; Q_{bio} is measured online, and $MLSS$ and SS_{RAS} are measured online and with lab-analyses.

2.2 Static mass balance

A static mass balance can be derived by solving (4) and (5) at steady-state,

$$\begin{aligned}
\frac{dV_{bio}}{dt} &= 0 = Q_{bio} + Q_{RAS} - Q_{tot} \Rightarrow Q_{tot} = Q_{bio} + Q_{RAS} \\
\frac{dMLSS}{dt} &= 0 = Q_{RAS} SS_{RAS} - (Q_{bio} + Q_{RAS})\, MLSS \\
0 &= Q_{RAS}(SS_{RAS} - MLSS) - Q_{bio} MLSS \\
Q_{RAS}(SS_{RAS} - MLSS) &= Q_{bio} MLSS \\
\Rightarrow Q_{RAS} = Q_{SMB} &= \frac{Q_{bio} MLSS}{SS_{RAS} - MLSS}
\end{aligned} \tag{6}$$

where Q_{bio}, $MLSS$ and SS_{RAS} are known parameters. Q_{bio} is measured online, and $MLSS$ and SS_{RAS} are measured online and with lab-analyses.

2.3 Function of the incoming flow and the water level in the bioreactor

The water exits the bioreactor over a rectangular weir. The flow rate exiting the bioreactor, Q_{tot}, can be estimated using Poleni's formula for rectangular weirs without contraction (Persson et al., 2014):

$$Q_{tot} = \frac{2\mu L \sqrt{2g}\,(h_{bio} - h_{ref})^{3/2}}{3} \tag{7}$$

where μ is a constant that accounts for frictions loss when the water exits the weir, L is the length of the weir, g is the gravitational constant, h_{ref} is the height from the bottom of the tank to the crest of the weir, and h_{bio} is the measured water level in the bioreactor (fig. 3). All variables are known.

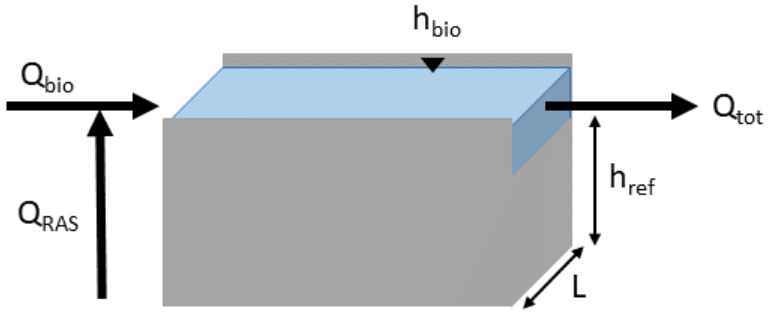

Figure 3. Illustration of the water exiting the bioreactor over a rectangular weir.

With the use of (7), (4), and simple geometry, it is possible to derive an expression for Q_{RAS} as a function of h,

$$
\begin{aligned}
\frac{dV_{bio}}{dt} &= Q_{bio} + Q_{RAS} - Q_{tot} \\
\frac{dV_{bio}}{dt} &= A_{bio}\frac{dh_{bio}}{dt} = Q_{bio} + Q_{RAS} - \frac{2\mu L\sqrt{2g}\left(h_{bio} - h_{ref}\right)^{3/2}}{3} \\
\Rightarrow Q_{RAS} = Q_{weir} &= \frac{2\mu L\sqrt{2g}\left(h_{bio} - h_{ref}\right)^{3/2}}{3} - Q_{bio} + A_{bio}\frac{dh_{bio}}{dt}
\end{aligned} \tag{8}
$$

2.4 Pump model

The behaviour of a pump can be described using its pump curve and system curve. The pump curve shows the relationship between the pressure and flow a pump generates at a certain frequency. The system curve contains two parts: the static head and frictional head loss. The intercept between the pump curve and the system curve gives the operational point from which the pumped flow and generated pressure can be retrieved. To change the flow rate, the operational point has to be moved which can either be done by changing the frequency or to change the static head or frictional head loss (Karassik et al., 2007).

The relation between the number of revolutions (n), flow rate (Q), pressure head (H), and required power (P) are described with the affinity rules (given that the diameter of the impeller is kept constant):

$$
\begin{aligned}
\frac{Q_1}{Q_2} &= \frac{n_1}{n_2} \\
\frac{H_1}{H_2} &= \left(\frac{n_1}{n_2}\right)^2 \\
\frac{P_1}{P_2} &= \left(\frac{n_1}{n_2}\right)^3
\end{aligned} \tag{9}
$$

If the flow rate, pressure, and power are known for a given n, these relations can be used to calculate Q, H and P for any n.

The system curve changes as the static head changes. The RAS pumps are located in a tank where the water level changes, which in turn changes the static head. Information about the pumps was used to fit a polynomial to the system curve. The frictional head loss was neglected. The system curves were assumed to only offset from each other depending on the water level, no change in shape.

The pump curves were assumed to be linear around the intercept with the system curve. Combining the polynomial for the system curve and the linear relationship describing parts of the pump curves give a second-order polynomial, which can be solved to find any flow rate for any static head and frequency. This method was previously used and implemented by Saagi et al. (2016). It was later revised for the Henriksdal WWTP by Blomstrand and Jemander (2017). Their work was used as a basis for the pump model. The pumps installed at Henriksdal WWTP are Flygt PL 7040 pumps. The pumps were

installed and tested during the autumn of 2019.

The RAS flow rate is possible to estimate using data from the plant. Required data is the water level in the tank where the RAS pumps are located, h_{RAS}, and the number of revolutions of the eight pumps, n_i. The available data from the plant is the frequency of the pumps which is related to the number of revolutions per minute,

$$n_i = \frac{120 f_i}{p} \tag{10}$$

where f_i is the frequency in Hz and p is the number of poles of the electrical drive.

2.5 Estimating the RAS flow rate

The median (11) and the mean (12) the of the four different calculations were calculated and used as a first combined estimate of the RAS flow rate,

$$Q_{median} = median(Q_{weir}, Q_{SMB}, Q_{DMB}, Q_{pump}) \tag{11}$$

$$Q_{mean} = \frac{Q_{weir} + Q_{SMB} + Q_{DMB} + Q_{pump}}{4}. \tag{12}$$

The median of four values was calculated as the average of the two middle values. Other methods such as using the maximum, minimum or a weighted average of the four flow rate estimates could have been used, but without knowledge about the true RAS flow rate it was deemed suitable to use the mean and median as a first test.

3 Default scenario

The four different calculations were implemented in the MBR model. A simulation of 21 days was run without disturbances in any input variable. The different estimates of the RAS flow were compared. The four calculations were deemed to be close enough (Figure 4). Only seven days are shown in Figure 4 for visibility purposes. The cyclic pattern was the same throughout the whole simulation period.

The results from this simulation were regarded as the ideal or default scenario to which the succeeding simulations were compared.

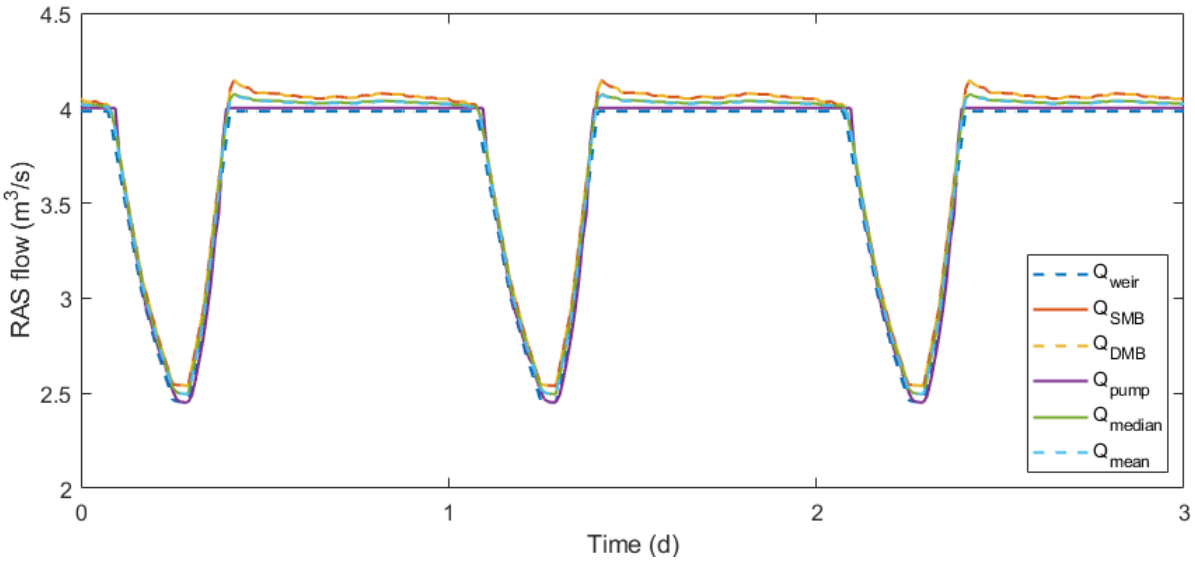

Figure 4. The simulated RAS flow rate using four different methods, and the final estimate of Q_{RAS}.

4 Adding disturbances to the input signals

To analyse how the soft sensor responds to disturbances in the input variables white noise with different standard deviations to match historic data was added to the signals. Historic data was analysed to find the average and standard deviation for each signal. Periods without abrupt changes were chosen for this purpose. The standard deviations used are presented in Table 1.

Table 1. Summary of the historic data set.

Signal	Mean	Standard deviation		Standard deviation / Mean
Q_{bio}	0.82	0.18	m^3/s	22%
h_{bio}	1.0	0.030	m	3%
$MLSS$	5 768	419	g/m^3	7%
SS_{RAS}	8 013	604	g/m^3	8%
h_{RAS}	1.2	0.18	m	15%

The output from the four different calculations of the RAS flow rate without noise in any input variables was regarded as the ideal case. Disturbances were first added to one signal at a time. The residuals were calculated and analyzed with regard to mean and standard deviation (Table 2). Unsurprisingly, disturbances in h_{bio} impacts the flow calculated over the weir. The water level is also used in the dynamic mass balance (as the change in the bioreactor volume) but it was only slightly impacted by the disturbances. The static mass balance and the pump model are independent of the level over the weir and were therefore not affected.

The dynamic mass balance was more affected than the static mass balance when disturbances were added to $MLSS$. The fluctuations in MLSS propagates in the dynamic mass balance as it takes into account the derivative of MLSS, which the static mass balance does not. Disturbances in SS_{RAS} also affect both mass balances. The disturbances in Q_{bio} affect both mass balances (static and dynamic) and the flow calculated from the weir. The pump model was unaffected as it does not account for the flow in to the bioreactor. The pump model was only affected by disturbances in the water level in the RAS pump tank (h_{RAS}). The input variable is only used in the pump model and therefore it was the only calculation that was affected when disturbances were introduced.

Table 2. Standard deviation of the residuals for the four different flow calculations when disturbances were added to one input variable at a time.

RAS flow	Q_{bio}	h_{bio}	$MLSS$	SS_{RAS}	h_{RAS}
Q_{weir}	0.18	1.7	-	-	-
Q_{SMB}	0.64	-	0.35	0.40	-
Q_{DMB}	0.64	0.000013	0.42	0.40	-
Q_{pump}	-	-	-	-	0.012
Q_{median}	0.32	0.020	0.18	0.21	0.0042
Q_{mean}	0.28	0.42	0.19	0.20	0.0030

Disturbances were then added to all signals to evaluate the response of each calculation when exposed to multiple disturbances. The disturbances were once again made up by random numbers with mean 0 and standard deviations as in Table 1. A simulation of 21 days was run. The output is shown in Figure 5. Only seven days are shown for visibility purposes.

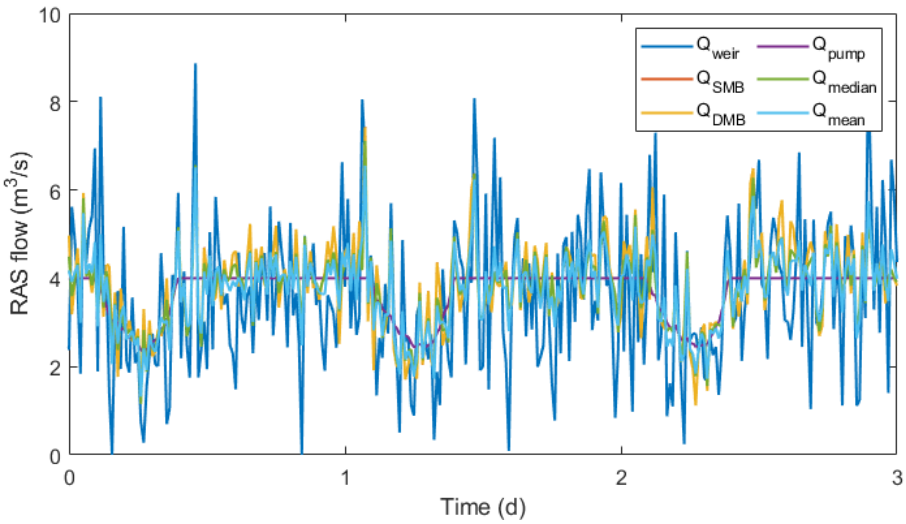

Figure 5. A three day period from a 21-day simulation with disturbances added to all input variables.

The mean and standard deviations of the residuals were calculated (Table 3, Figure 6). When adding multiple disturbances, the residuals are quite large for all estimates except the pump model. The residuals of Q_{weir} mostly stems from the disturbances in h_{bio}, whereas they are more likely explained by a combination of disturbances in several input variables (Q_{bio}, $MLSS$, SS_{RAS}) for the mass balances (SMB, DBM).

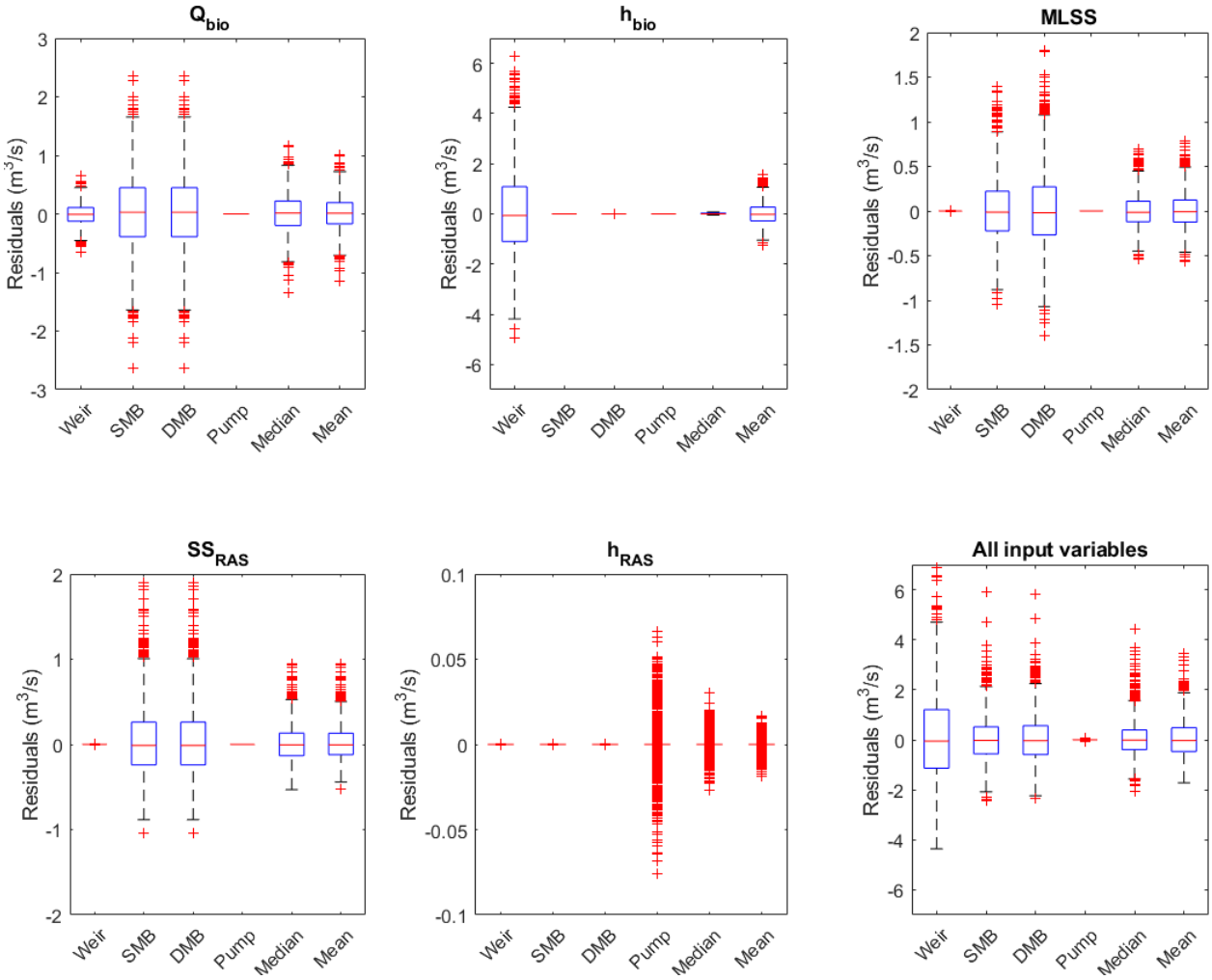

Figure 6. Residuals when adding disturbances to one variable at a time. Note the different ranges on the y-axis. The weir calculation is most sensitive to disturbances in h_{bio} and the dynamic mass balance (DMB) is sensitive to disturbances in MLSS. When adding disturbances to all input variables at the same time, the residuals are greatest for the weir calculation followed by the two mass balance models. Median and mean refers to the median and mean as equations (11) and (12).

Table 3. Residuals when adding multiple disturbances.

$\mathbf{Q}_{RAS}$	**Mean** m^3/s	**Std. dev.** m^3/s	**Average flow** m^3/s	**Std. dev. / Average flow**
Q_{weir}	0.080	1.7	3.76	46%
Q_{SMB}	0.036	0.88	3.79	23%
Q_{DMB}	0.037	0.91	3.79	24%
Q_{pump}	0.00020	0.012	3.69	0.33%
Q_{median}	0.045	0.72	3.77	19%
Q_{mean}	0.038	0.73	3.76	19%

The residuals all have means close to zero but the standard deviations are in general quite large (Table 3). The weir calculation is most sensitive to disturbances. The standard deviation of the residuals is approximately 46% of the average flow rate calculated over the weir. This is also seen in Figure 5 where the output is fluctuating significantly. It should however be noted that none of the signals were filtered since the purpose was to examine the effect of disturbances. A more realistic approach (to later be implemented) would be to filter the input data to reduce the fluctuations.

5 Using historic plant data

Data from the MBR line at Henriksdal WWTP were extracted for the period 2021-06-09 - 2021-06-30. The data set included; the incoming flow rate (Q_{bio}), water level in the bioreactor (h_{bio}), MLSS in the bioreactor ($MLSS$) and SS in the RAS flow rate (SS_{RAS}). The frequency of the RAS pumps was not accessible at the time. The pump model described in this work was therefore not tested with historic data. Instead, the RAS flow rate calculated in the control system (also based on pump characteristics and frequency) was used for comparison (Q^*_{pump}). This model does however not account for the change of water level in the RAS pump tank. The used data is shown in Figure 7.

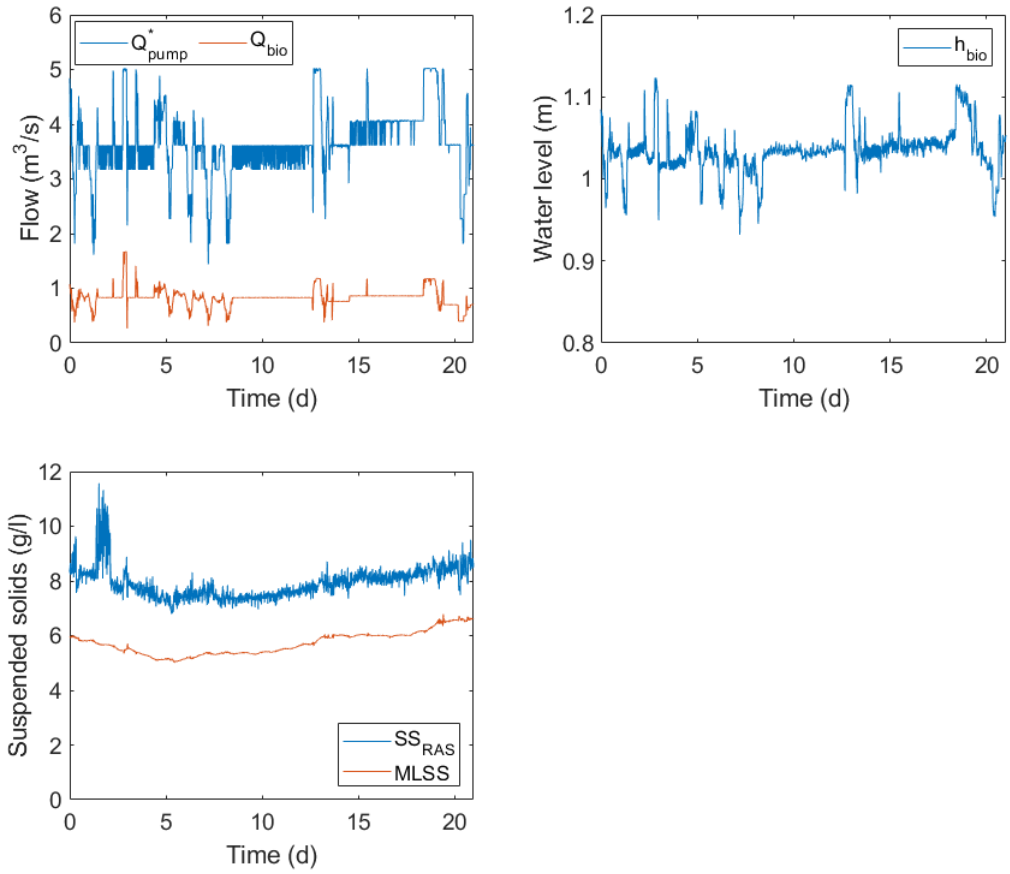

Figure 7. The raw data used in the soft sensor. Q^*_{pump} is the RAS flow rate calculated in the control system.

The extracted data was run through the soft sensor. The input signals were filtered by applying a moving average of 3 hours. The results are shown in Figure 8. What is obvious is that the two mass balance models give very similar results. Q_{weir} and Q^*_{pump} are consistently higher than the mass balance based calculations. Towards the end of the examined period there is an almost constant offset between the two groups.

When comparing Q_{weir} and Q^*_{pump} it can be concluded that they are quite similar to each other. An interesting notion is that Q_{weir} is lower than Q^*_{pump} from day 3 to 9, then follows a period where they are approximately equal but where the flow peaks are higher in Q_{weir} than in Q^*_{pump}. This could indicate that Q_{weir} is more sensitive to variations in the input variables than Q^*_{pump}, which coincides with the results from the sensitivity analysis. It is however difficult to jump into conclusions based on this since there is no 'true' flow rate to validate with and no knowledge on whether all sensors were fully functional during this period of time.

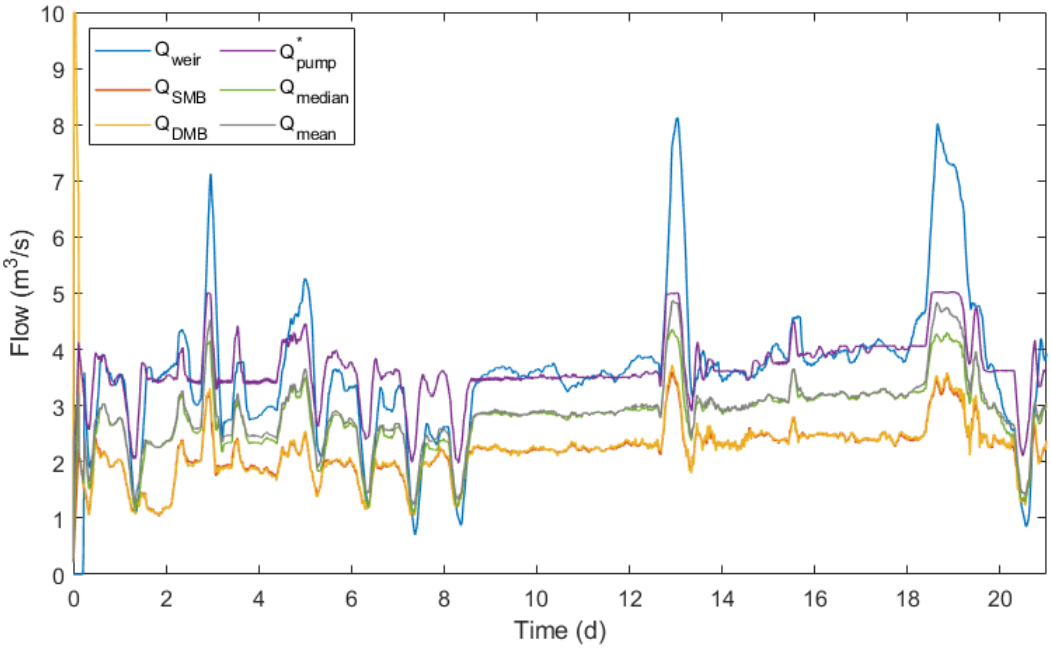

Figure 8. Simulation with filtered historic input data. Q^*_{pump} is the RAS flow rate calculated in the control system.

To summarize the results a bit more the maximum and the minimum at each time step was plotted together with the median flow rate (Figure 9). As is seen, the results cover quite a large span which makes it difficult to estimate one ”true” RAS flow rate.

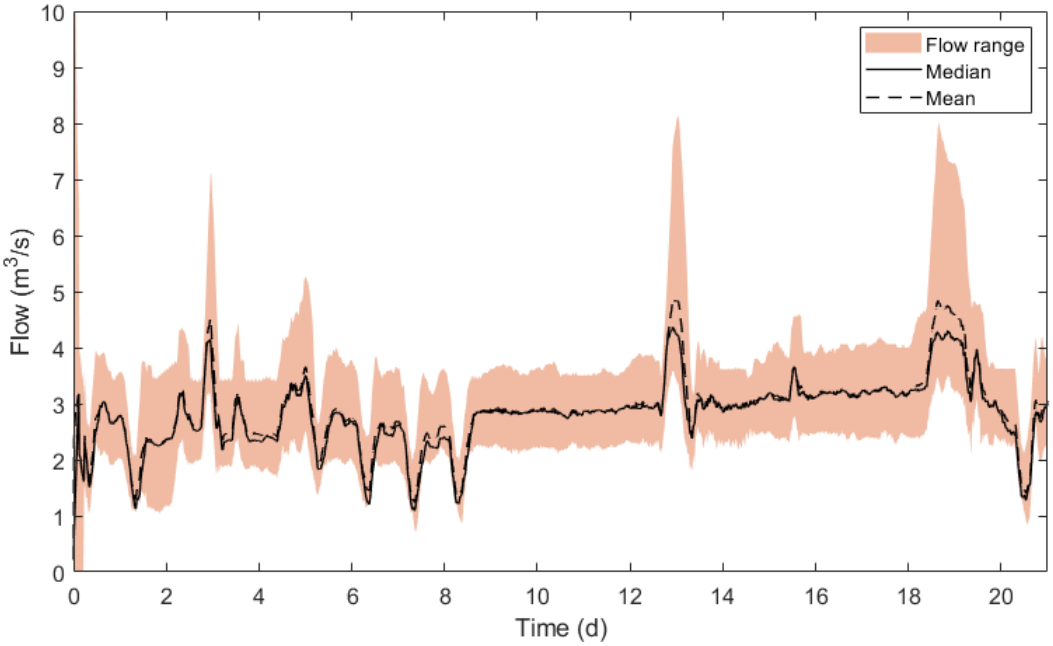

Figure 9. Minimum and maximum flow at each time step, together with the median and mean, shows the large spread in the four different estimates.

Out of curiosity, the ratios between the two mass balance models and the pump flow rate

from the control system (which was less prone to disturbances than Q_{weir}) were calculated and plotted. The ratios are around 0.6 throughout most of the period (Q_{SMB}/Q_{pump}*: mean = 0.59, standard deviation = 0.067, Q_{DMB}/Q_{pump}*: mean = 0.59, standard deviation = 0.069). An explanation to this rather constant offset is yet to be found.

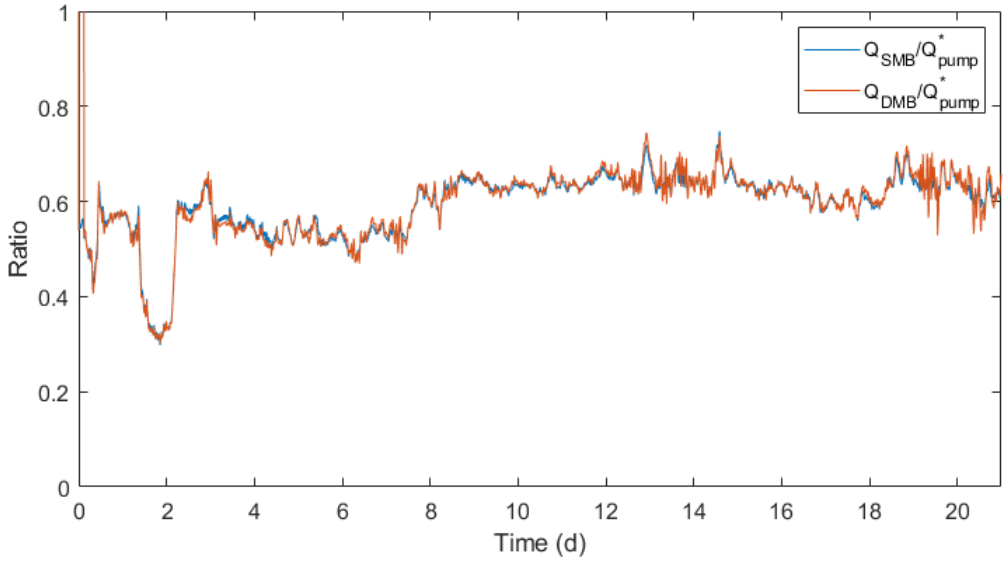

Figure 10. The ratios between the two mass balance models and the calculated pump flow rate from the control system.

6 Discussion

This simulation study investigated whether it was possible or not to create a soft sensor for the return activated sludge flow rate (RAS flow) at Henriksdals WWTP. Four different models were used, evaluated and compared to each other, first using simulated data with and without disturbances, and later with real historic data from the treatment plant. The weir calculation was most sensitive to disturbances when using simulated data. This could explain why it deviates from the more stable pump model in an irregular way when feeding the soft sensor with historic data. The weir model is apparently quite sensitive to changes in water level. It was also noted that the model was sensitive to the choice of the model parameters (h_{ref}, L and μ) but it was not quantified. A more extensive uncertainty analysis and sensitivity analysis should be performed on the four different models individually so as to estimate how large uncertainties one could expect from each calculation. That might provide insight to what results to trust.

Based on the results in this study it is impossible to decide on a 'true' RAS flow rate at Henriksdals WWTP. Figure 9 shows the large range between the maximum and minimum estimate at all time steps but it is not possible to determine which flow is most or least accurate. Since there is no flow rate available to validate the calculations one can only guess which model is most accurate. An uncertainty analysis could help to prioritize between the four estimates.

There is a quite large offset between the mass balance models and the pump flow rate from the control system but they all follow the same general pattern. Looking at the difference between the mass balances and the pump flow there almost seems to be a constant offset. The mass balances equals approximately 60% of the pump flow. An explanation to this has not been found. It could be that the pump model overestimates the RAS flow. The pump model assumes that the pump has a certain efficiency which might not coincide with reality. The pump model in the control system (the one that was used with historic data) does not account for the water level in the pump tank which also might affect the results. To what extent is not known and will probably not explain the whole offset though. Using this as an explanation would imply that Q_{weir} is incorrect but tuning the model parameters is possible if a 'true' flow rate was determined. One could on the other hand argue that the weir and pump flows are correct and that the mass balance models underestimate the flow rate. Both mass balance models are simplifications of reality and based on assumptions. The MLSS and SS_{RAS} sensors could be faulty or there might be unknown flows or interactions that was not accounted for in this study.

The decision to use the median and mean flow as Q_{RAS} may not be the best approach for estimating the flow rate. It could be considered to add weights to the different flows, but again, this is difficult, if not impossible, to determine without knowing what data to calibrate against.

Although this study did not result in a comprehensive way of estimating the RAS flow rate, the method could be used further for fault detection. If this was to be regarded as the 'default' case - where $Q^*_{pump} \approx Q_{weir}$ and $Q_{SMB} \approx Q_{DMB}$ - future estimates could be evaluated and compared to these.

7 Future research

Based on the results of this study, the following would be valuable to further investigate:

- Perform uncertainty analysis and local and global sensitivity analysis with more advanced methods to estimate the contribution from each input variable and parameter in the four different calculations to determine which estimate is least/most sensitive. Based on this, possibly redefine how the RAS flow rate should be estimated.
- Search for an explanation to the offset between Q_{pump}, Q_{weir} and Q_{SMB}, Q_{DMB}, possibly by analysing a longer time period and see if the offset between Q_{pump} and the mass balance models has been and remains constant.
- Use the different calculations to detect measurement faults in the flows or the input variables by comparing them to a decided 'true' flow rate.
- Test the pump model with historic plant data to quantify what influence the change in water level in the RAS tank has on the flow rate estimate.

References

Blomstrand, P. and Jemander, R. (2017). *Systemteknisk studie av pumpstyrning på Henriksdals nya reningsverk*. MSc thesis. Uppsala university. Department of Information Technology. Sweden, http://www.w-program.nu/filer/exjobb/Patrik_Blomstrand_och_Rasmus_Jemander.pdf.

del Olmo, F. H., Gaudioso, E., Duro, N., and Dormido, R. (2019). Machine learning weather soft-sensor for advanced control of wastewater treatment plants. *Sensors*, vol. 19(14):pp. 3139.

Haimi, H., Mulas, M., Corona, F., and Vahala, R. (2013). Data-derived soft-sensors for biological wastewater treatment plants: An overview. *Enviromental Modelling & Software*, vol. 47:pp. 88–107.

Hammer, M. J. S. and Hammer, M. J. J. (2014). *Water and Wastewater Technology*. Pearson Education Limited, Essex, UK, 7th edition.

Karassik, I., Messina, J., Cooper, P., and Heald, C. (2007). *Pump Handbook*. McGraw-Hill Education, New York, USA.

la Cour Jansen, J., Arvin, E., Henze, M., and Harremoës, P. (2019). *Wastewater Treatment - Biological and Chemical Processes*. Polyteknisk Forlag, Copenhagen, Denmark, 4th edition.

Mali, B. and Laskar, S. (2020). PLS-based multivariate statistical appraoch for soft sensor development in WWTP. Shreesha, C. and Gudi, R.D. (eds.). *Lecture Notes in Electrical Engineering, Proceedings of the 15th annual Control Instrumentation System Conference (CISCON)*, Oct. 26-27, Manipal, India. pp. 123-131.

Persson, J., Fridell, K., Gustafsson, E.-L., and Englund, J.-E. (2014). *Att räkna på vatten - en formelsamling för landskapsingenjörer*. (Report 2014:17). Alnarp, Sweden: Swedish University of Agricultural Sciences.

Pisa, I., Santín, I., Vicario, J. L., Morell, A., and Vilanova, R. (2019). ANN-based soft sensor to predict effluent violations in wastewater treatment plants. *Sensors*, vol. 19(6):pp. 1280.

Saagi, R., Flores-Alsina, X., Butler, D., Gernaey, K., and Jeppsson, U. (2016). Catchment & sewer network simulation model to benchmark control strategies within urban wastewater systems. *Enviromental Modelling & Software*, vol. 78:pp. 16–30.

Stockholm Vatten och Avfall (2017). *Tekniskt nedslag i Stockholms framtida avloppsrening*. http://www.stockholmvattenochavfall.se/globalassets/sfa/pdf/informationsbroschyrer/tekniskt-nedslag-i-stockholms-framtida-avloppsrening, [2021-10-08].